

# ELECTRON TRAPS AND TURBULENCE DIAGNOSTIC

M. Cavenago\*, INFN/LNL, Legnaro, Italy,

G. Bettega, F. Cavaliere, R. Pozzoli and M. Romè, INFN-Milano, Italy

## Abstract

In the electron trap Eltrap both trapped and propagating beams can be studied. Beam structures in the transverse plane  $xy$  were successfully detected. A set of cylindrical electrodes controls the beam. The addition of an external electron source, controlled by a laser, makes ns electron bunches now possible. A system to dump the electron beam off axis is here described. Faster diagnostic and control methods can be tested. In particular, Thomson scattering diagnostic of beam structures can be tested. Preliminary beam images are shown.

## INTRODUCTION

The electron trap ELTRAP[1] is a versatile facility to study propagation and storage of electron beams at a very low voltage. The central block is a 1.5 m long solenoid (uniformity in the  $10^{-4}$  order over 1 m) well aligned with a system of 12 cylindrical electrodes whose voltages can be independently controlled in the  $\pm 100$  Volt range (at a  $10^7$  sample/s), see Fig. 1. This allows to study the injection, storage and extraction of electrons; several structures and instabilities were observed[2, 3, 4]. These structures, named vortex crystals, have analogies with several phenomena, ranging from meteorology to superconductivity[5]. In another operation mode, the electron beam is propagated through, using the magnetic field  $\mathbf{B} \cong B_0 \hat{z}$  as a control parameter of the evolution due to nonlinear dynamics of the  $(x, y)$ -section of the beam: here  $z$  is the solenoid axis and  $z = 0$  the solenoid center. Beam radius ranges from 2.5 mm to 38 mm, depending on the source used.

It was appealing to use this system to model Thomson laser diagnostic and rf photoinjectors, at much lower voltage and power density, keeping the perveance  $IV^{3/2}$  fixed. This experiment requires to bunch the electron source faster, on a ns scale; two new modules were inserted at the opposite side of the solenoid. One module houses the external source, with an additional solenoidal  $B^s$  and an input viewport for the laser L1 which controls the source pulse. Source is held to a voltage  $V_s$  (from -4 kV to -10 kV, where ground is the vacuum chamber) and accelerating gap is 12 mm long. The other module houses the input for laser L2, an array of six photomultiplier tubes (PMT) to detect the light backscattered from the electron beam and an electron dump system, with a deflector to deviate electrons far away from PMTs. Two scrapers shield these PMTs from the ultraviolet (UV) emitted at the e-dump. All parts are assembled and ready for commissioning.

\*cavenago@lnl.infn.it

Unfortunately a failure of the L1 laser compelled us to run in a CW mode, without testing the Thomson diagnostic and the dump module, so results with the external source only are presented here. Rest of the paper is so organized: the beam optics design of the electron dump is discussed in the next section, while the external electron source set-up is discussed in the last section, also reporting results on the annular beam produced.

## ELECTRON DUMP AND OPTIC DESIGN

The laser L2 axis crosses the  $z$ -axis at  $z_c = 0.2$  m, making an angle of 10 mrad. Assuming a beam radius of 2.5 mm and similarly for the laser (a 4 ns pulse, 0.425 J at 532 nm), we limit the interaction region to  $z_c \pm 0.25$  m. Since the uniform magnetic field opposes to beam deviation, the deflector has to be located after the iron ring I4, which sits near the plane  $z_I \equiv 0.74$  m and which reduces  $\mathbf{B}$ . We also add two iron shims I5 and I6, to further deviate the magnetic field lines. We optimized optics and e-dump position for the fringing field corresponding to  $B_0 = 0.1$  T, since this is rarely surpassed in experimental conditions. Dump stays around the  $z = z_v = 1.1$  m plane, where 8 lateral flanges CF63 are provided; some phosphors PL may be placed there, at  $r \geq r_D = 0.125$  m. Deflection voltages for a fixed dump position increases with  $B_0$ , so the  $B_0 = 0.1$  T case give maximum requests. In simulations we considered two examples  $V_s = -4$  kV as planned in first tests, and  $V_s = -8$  kV as the low perveance limit, of limited interest.

The deflector centered at  $z_D = 0.842$  mm is made of two cylinder sectors, inner radius  $R_d = 45$  mm, angular span  $\pi/2$ , length 124 mm, with positive  $V_+$  and negative  $V_-$  voltages. The diverging magnetic field is  $B_z(0, 0, z_D) \cong 0.3B_0$  at its center.

Central trajectory simulations[6] for  $z \geq 0.74$  m (fig. 2) show that the unipolar deflector scheme that has  $V_+ = 0$  and  $V_- = -V_n$  requires  $V_n = 6.92$  kV, (respectively 10.7 kV and 12.4 kV) for  $V_s = -4$  kV (respectively -8 kV and -10 kV) in order to deflect the beam in the dump ports. There is a  $\theta$  angle between the beam plane and the direction of  $\mathbf{E}$  in the deflector; without magnetic field, we would have  $\theta = 0$ ; for fig. 2A case,  $\theta = 99^\circ$ . A bipolar deflector will require about  $V_+ = -V_- \geq V_n/2$ . For allowing experimental flexibility,  $\mathbf{E}$  can be rotated in steps of  $9^\circ$  and viewports PL can be placed at  $45^\circ$  steps. To scan a large and continuous  $B_0$  range, vacuum opening may be necessary to rotate the deflector.

Beam simulations, assuming a  $b = 2.5$  mm beam radius and a parallel beam at magnet exit  $z = z_I$  and a  $I_b = 1$  mA current, confirm dumping of the whole beam. Space

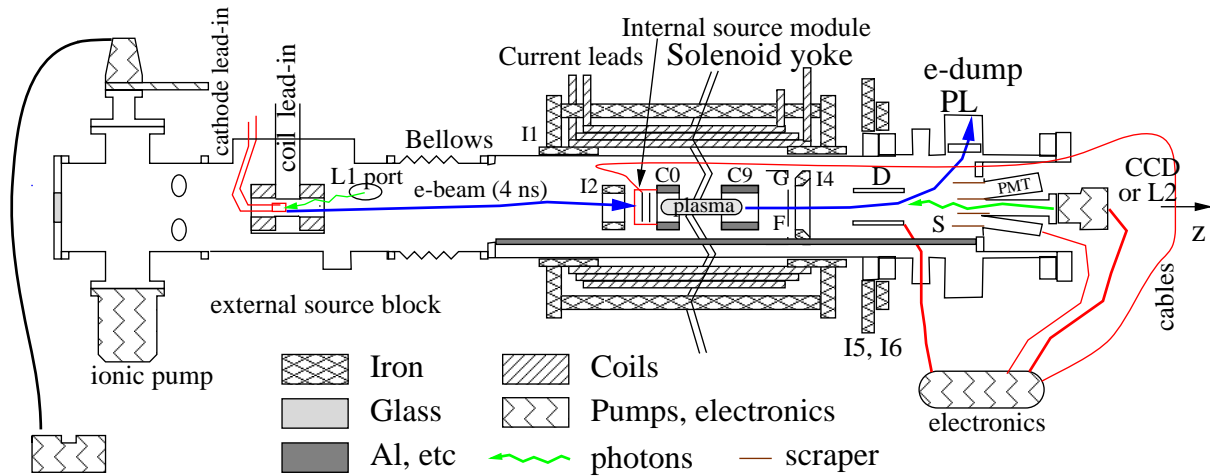


Figure 1: Overview of the final set-up, not to scale. Note electrodes (C0 ..C9), shims (I1 .. I6), phosphors P and PL, laser ports L1 and L2 and scraper system S. Electrons will be deviated by deflector D

charge is fairly negligible, since the self electric field (for  $V_s = -4$  kV) is

$$E_r^{self} \leq -\frac{(m/e)^{1/2}}{23^{3/2}\pi\epsilon_0} \frac{I_b}{b\sqrt{|V_s|}} = -160\text{V/m} \quad (1)$$

which is much smaller the peak deflection field

$|V_n|/2R_d = 55\text{kV/m}$ . Beam is distorted and magnified at dump, as apparent from fig 2. If this large beam size at the dump will make UV scrapers not effective, it may be desirable to reduce the beam size at dump. As a working hypothesis, we assumed that is possible to prepare a distorted beam at  $z = z_I$ : result of a particularly effective combination of quadrupole and beam rotation is shown fig 3. To this purpose, substitution of the second last electrode C8 with combined Glaser-quadrupole lens is being investigated.

### THE EXTERNAL SOURCE

A pair of coil included into the source assembly generate a solenoidal magnetic field with a maximum  $B^s$  at source cathode and a FWHM of 5 cm; we have about  $B^s/I_s = 40$  G/A with  $I_s$  the current in the coils (rated up to 2.5 A). The external source is aligned to its vacuum chamber within a 0.1 mrad accuracy and is connected with bellows to the

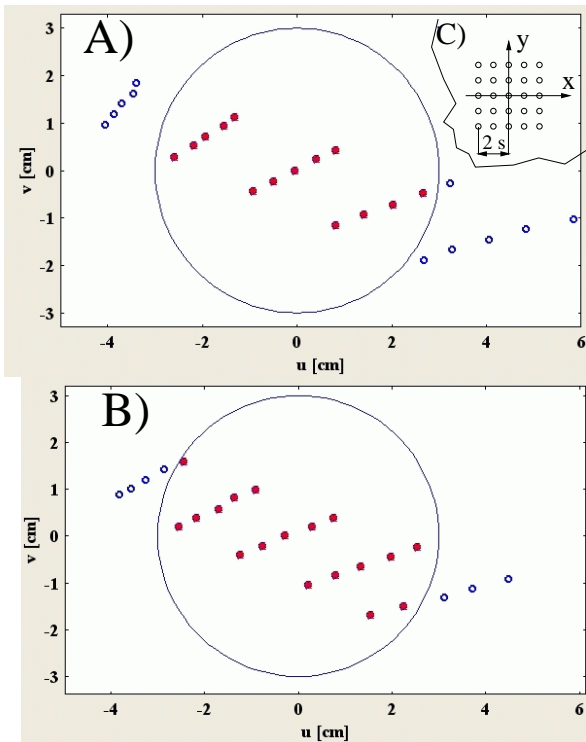


Figure 2: Electron beam impact points on the plane  $uv$  that includes the phosphor PL face (large circle) for different source voltages  $V_s$ : A) -4 kV; B) -8 kV. Note that  $u = z - z_v$  with  $z_v = 1.1$  m. Electrons were assumed to start perpendicularly to the the plane  $z = z_I = 0.74$  m, distributed on a  $5 \times 5$   $xy$  grid (shown in C) with  $s = 1$  mm spacing.

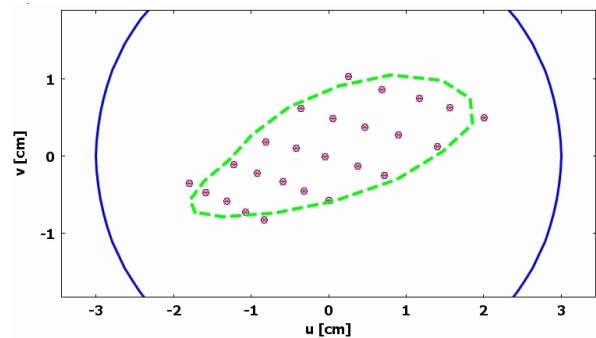


Figure 3: Dump of properly preconditioned beam. A rotating beam (60 MHz frequency) was considered and a quadrupole map (magnifying  $x$  by 1.8 times,  $y$  by 0.2 times) was applied at  $z_I$ ; green dashed line is the contour of a initially circular beam with 2.5 mm radius. Other conditions as in fig 2.A.

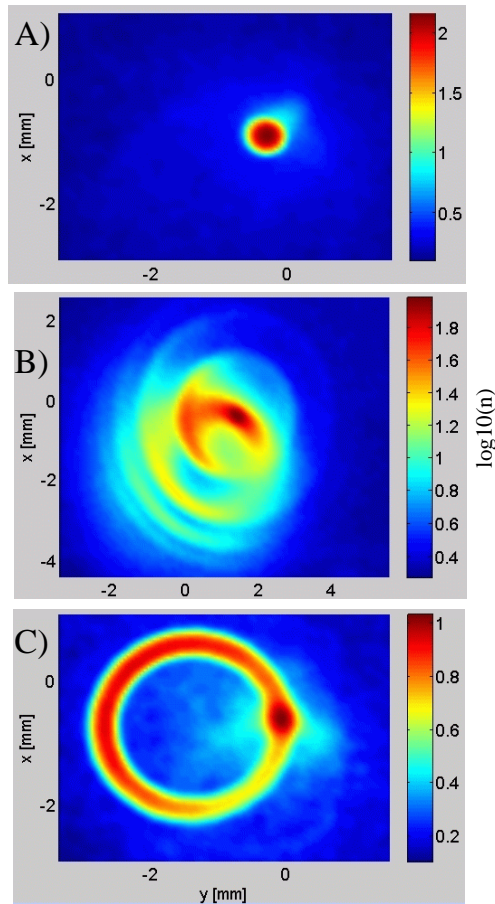


Figure 4: Beam images (color scale  $\propto \log_{10}(n)$  where  $n$  is light density with a minimal background subtraction): A) focused spot; B) concentric rings; C) annular beam.

vacuum chamber of the main solenoid where an uniform  $B_z = B_0$  magnetic field is obtained, so that any discrepancies of the magnetic axes can be adjusted.

Source consists of a flat thermionic cathode (a 6.3 mm diameter 10 mm long M-type dispenser), with emission from  $T_c = 1150$  to 1300 K, in CW mode; a collimator placed over the source (with a 0.1 mm gap) reduce beam radius to  $r_s = 2.5$  mm. Since  $B_0 \gg B_s$  a paraxial and laminar transport can be expected. The longitudinal bunching is then well separated from the transverse motion.

In pulsed mode[7], the laser L1 entering from a CF16 side port at  $40^\circ$  with  $z$ -axis impinges onto the warm cathode, and can produce a 4 ns electron bunch (fig. 2): emission is mainly photoelectric, but efficiency is enhanced since half a barium monolayer is dynamically maintained by cathode heating at  $T_c \cong 1000$  K.

An UV laser (337 nm, 0.26 mJ per pulse, 30 Hz, 0.5 mrad divergence) is needed for the photoelectric effect, but a much lower power red light laser was planned for alignment. Now laser L1 is directly pointed trough the CF16 port. Keeping the electrode from C1 to C12 to ground and  $B_0 \neq 0$ , beam images can be recorded at the phosphor F (placed instead of the electron dump). Images may be averaged by software; the phosphor saturation and the image

download times from CCD slow the acquisition to 2 image/s. A signal  $V_d$  is detected by a pickup (capacitatively coupled to source voltage  $V_s$ ), followed by some SMA attenuators (23 dB maximum) and a buffer amplifier (about 52 dB gain). This is averaged by a digital oscilloscope, triggered by the laser circuitry with a 700 ps jitter. A mechanical shutter allows to take the reference measurement, for subtracting the background (well visible and due to laser power electronics).

During pulse, the source current is supplied by the nearby capacitances, estimated to be 70 pF (with about a 20 nH inductance) including the detector itself, while the power supplies are decoupled by a section of the connection cable, with inductance well above 1  $\mu$ H. So voltage pickup  $V_d$  can thus give a measure, even if distorted, of source operation, and some further calibration is needed. A Rogowsky coil is now in preparation. Unfortunately, the failure of laser L1 prevented these calibrations.

CW commissioning of external source was still possible. Cathode is capable of maintaining a 1173 K temperature with 4.5 W ( $I_f = 1.36$  A,  $V_f = 3.3$  V) when thermally isolated. Due to the source electrode alignment assembly, this increase to 7 W as measured ( $I_f = 1.7$  A,  $V_f = 4.4$  V). A beam current of few tens of  $\mu$ A is enough for bright images. Thermal equilibrium requires rather long times (up to 300 s) due to masses and nonlinearities involved, as apparent from  $V_f$  and from the current emitted.

A well focused spot was obtained when  $B_z^s \geq 20$  G,  $B_0 \geq 0.02$  T, see Fig. 4.A: this proves a satisfactory alignment, and a good transport. By decreasing  $B_0$  to 0.015 T, preliminary observation of beam structures as in Fig. 4.B were possible: secondary rings are visible, with an  $m = 1$  modulation of the local intensity (better seen from 3D plots). Keeping  $B_0 = 0.03$  T constant and reversing the sign of  $B_z^s$  we see that transported beam becomes an annulus, with still a peak  $P_1$  on its periphery (fig Fig 4.C, for  $B_z^s = -60$  G). By manually sweeping  $B_z^s$  from -60 G to +60G, the annulus rotates around  $P_1$  and expands, reaching its maximum radius about when  $B_z^s$  crosses zero; by the end of sweep, annulus has shrunk and disappears under the fig 4.A peak.

In summary, CW operation of the system were demonstrated. Completion of some automation and repair of L1 is needed for full operation.

## REFERENCES

- [1] M. Amoretti et al., Rev. Sci. Instrum. **74** (2003) 3991.
- [2] G. Bettega, F. Cavaliere, M. Cavenago, A. Illiberi, R. Pozzoli, M. Romè, *Plasma Phys. Control. Fusion*, **47**, (2005) 1697.
- [3] M. Cavenago et al., Proceedings EPAC 2006, 2490
- [4] G. Bettega et al., Phys. Plasmas, **13** (2006) 112102
- [5] D. H. E. Dubin and T. M. O'Neil, Rev. Modern Physics 71 (1999) 87.
- [6] *Comsol Multiphysics 3.3*, see also <http://www.comsol.eu>
- [7] D. W. Feldman et al., Proceeding of the 2001 PAC (IEEE, Piscataway, 2001), 2132